



# Evaluation and analysis of perlite and municipal wastewater sludge (biosolids) from three wastewater treatment plants in East Texas, USA

Kefa K. Onchoke · Oluwadamilola O. Fateru ·  
Robert B. Friedfeld · Paul W. Weatherford

Received: 20 May 2020 / Accepted: 15 January 2022 / Published online: 24 January 2022  
© The Author(s), under exclusive licence to Springer Nature Switzerland AG 2022

**Abstract** Municipal wastewater sludge (also known as biosolids) is produced in large quantities from wastewater treatment plants (WWTPs). Traditionally, analyses of biosolids revealed the presence of inorganic (including metals) and organic contaminants which pose health concerns to man and the environment. This study investigated physical-chemical parameters and comparative element concentrations (Ag, Al, As, B, Ba, Ca, Cd, Co, Cr, Cu, Fe, Hg, K, Mg, Mn, Mo, Ni, P, Pb, S, Se, Zn, V, Na, S, and P) in biosolids and composted wastewater sludge (CWS) from Nacogdoches Wastewater Treatment Plant (NWWTP), Lufkin Wastewater Treatment Plant (LWWTP), and Angelina-Neches

Compost Facility (NCF) in East Texas (USA). In addition, concentrations in perlite, a hydroponic material, were determined via Fourier transform infrared spectroscopy (FT-IR), scanning electron microscopy/energy dispersive X-ray diffraction (SEM/EDX), inductively coupled plasma-optical emission spectroscopy (ICP-OES), X-ray diffraction (XRD)), and thermogravimetric (TGA) analysis. Via ICP-OES analysis, metal concentrations in biosolid samples were similar. Macroelement amounts followed the order: NWWWS  $\approx$  LWWS > NCS > perlite. Notably, concentrations in biosolids, CWS, and perlite are below recommended USEPA and WHO maximum ceiling levels. The pH of biosolid samples was determined between 5.33 and 6.74. The weight losses of 6–19% wt at  $\sim$  300–700 °C are attributed to volatile compounds and inorganic metal oxides. From environmental and circular economy perspectives, this study shows biosolids to be safe, and potential recycling can be encouraged for use in soil amendments. This finding could find impetus to design of much better WWTPs which improve removal efficiencies and encourage recycling of biosolids.

**Supplementary information** The online version contains supplementary material available at <https://doi.org/10.1007/s10661-022-09794-z>.

K. K. Onchoke (✉) · O. O. Fateru  
Department of Chemistry & Biochemistry, Stephen  
F. Austin State University, Box 13006 – SFA Station,  
Nacogdoches, TX 75962-13006, USA  
e-mail: Onchokekk@sfasu.edu

R. B. Friedfeld  
Department of Physics, Engineering & Astronomy,  
Stephen F. Austin State University, 1901 Raguet St North,  
Box 13044, Nacogdoches, TX 75962, USA

P. W. Weatherford  
Department of Agriculture, Soil, Plant and Water Analysis  
Lab, Stephen F. Austin State University, P.O. Box 13025  
SFA Station, Nacogdoches, TX 75962-3025, USA

**Keywords** Spectroscopic characterization ·  
Biosolids · Wastewater treatment plants (WWTP) ·  
Neches Compost Facility (NCF) · Perlite · TGA

## Introduction

Wastewater treatment plants produce large amounts of solid waste with high organic matter content called biosolids or wastewater sludge (Fullana et al., 2004) that is disposed to the environment. In the USA, land application is the major use of sludge, which helps reduce the need for chemical fertilizers (Xue et al., 2015). Approximately 8 million dry metric tons of biosolids are produced annually in the USA, about half of which is applied to land as fertilizer, and the other half is either incinerated or deposited in landfills (Peccia & Westerhoff, 2015; Sherburne et al., 2016; USEPA, 2006). The processes of disposing the biosolids depend largely on the class of biosolids produced. The generation and treatment of wastewater processes to produce biosolids for useful purposes are important for the health of humans, animals, or plants. However, concerns abound on the applications of biosolids as soil amendments. The uptake of the macroelements or microelements by plants (and their consumption) may lead to accumulation of metals in the environment (Yang et al., 2014).

Numerous studies have characterized biosolids by using chromatographic or spectroscopic techniques including nuclear magnetic resonance spectroscopy (NMR) (Piotrowski et al., 1984; Smernik et al., 2003), X-ray absorption near edge structure spectroscopy (XANES) (Hettiarachchi et al., 2006; Shober et al., 2006), transmission electron microscopy (TEM) (Yang et al., 2014), Fourier transform infrared spectroscopy (FTIR) (Onchoke et al., 2018a), Raman spectroscopy, ion chromatography (IC) (Onchoke et al., 2018a), scanning electron microscopy (SEM), and thermochemical methods (Barneto et al., 2009; Kreutter et al., 2019). Characterization of biosolids is important for assessing the impact of land-applied biosolids to plants and humans. Examination of pollutants or metal concentrations in biosolids enables understanding possible exposure pathways to the environment, designing of disposal or recycling methods (Cheng et al., 2020), and/or the instituting and enacting steps that can reduce potentially harmful routes.

The global worldwide challenges and in the USA focus on cognizance of various emerging pollutants including perfluoralkyl sulfonates (PFAS) laden in biosolids (D'Agostino & Mabury, 2017). Thus, government agencies and research centers continue to

quantify, assess, and pursue measures geared towards reducing effects of these pollutants. Such pollutants interact with metals that occur in different speciated forms. The microscopic and macroscopic parameters necessitate the continuous studies of biosolids-metal interactions.

As population increases and city municipalities receive more city dwellers, the need for more WWTPs becomes urgent. In the USA and other developed countries, about 80% of domestic WW is treated centrally via sewerage in WWTPs. The sewage sludge produced is mainly applied for agricultural purposes, disposal via land filling, and/or incineration for energy recovery (Cheng et al., 2020). The challenges and necessity of increasing WWT facilities include the need for more land use with city development, and new facilities that are capital and energy intensive (Ghimire et al., 2021). Thus, WWTPs become useful resources for cycling water, energy, and nutrients. The need for the circular economy, defined as “keeping materials and products in the economy as long as possible by promoting recycle and reuse” (Ghimire et al., 2021), is necessary. The goal is to extract or retrieve organic carbon, phosphorus, nutrients, low-grade heat, and other recoverable products such as rare earths (Westerhoff et al., 2015; Yang et al., 2014).

Trends for wastewater management and recycling economy, therefore, include a need to ensure utilization of the many resources prevalent in wastewater products, and specifically, biosolids. Other challenges are the removal of inorganic and organic pollutants including emerging pollutants such as pesticides, metals, pharmaceuticals, nanoparticles, and microplastics (Keller et al., 2020). Although WWTPs are efficient in the removal of pollutants, designing analytical methods for detection of pollutants at low ppt level are also essential.

In East Texas (USA), recent studies investigated the metal content of biosolids (Onchoke & Fateru, 2021; Onchoke et al., 2018a). Although previous analysis for NWWTP and LWWTP (Onchoke et al., 2018a) was reported, a re-evaluation of biosolids from WWTPs was deemed necessary to provide baseline data for comparison with reported studies. Conversely, there is paucity of reports of CWS from Angelina-Neches Compost Facility (NCF) on metal concentrations and structural composition. The present study used multi-pronged spectroscopic

techniques to characterize biosolids collected from Lufkin or Nacogdoches wastewater treatment plants (LWWTP and NWWTP) and the Angelina-Neches Compost Facility (NCF). Inductively coupled plasma optical emission spectroscopy (ICP-OES) was employed to quantitate Ag, Al, As, B, Ba, Ca, Cd, Co, Cr, Cu, Fe, Hg, K, Mg, Mn, Mo, Ni, P, Pb, S, Se, Zn, V, and Na in biosolid samples. The morphology, particle size, and crystalline nature of the biosolid samples were determined using scanning electron microscopy (SEM) and X-ray diffraction (XRD). The % loss of mass (or decomposition) of biosolid samples was also provided using thermogravimetric analysis. In addition, it was the objective of this study to quantitatively assess perlite—a hydroponic material used for soils and/or biosolids amendments. Thus, spectroscopic inter-comparisons of biosolids, CWS, and perlite were investigated.

In this paper, we present a multi-pronged spectroscopic study for detection and quantifying metal content in wastewater biosolids from three WWTPs in East Texas and a hydroponic material (perlite). There are three aspects to this study. First, the need to determine the concentration of metals is critical to assessing toxic levels and possible risks when biosolids are used as soil amendments. Second, the evaluation of the efficiency of the WWTPs in removal of metals, and metal content in a commercially used composted wastewater sludge (soil therapy compost), and the well-known soil amendment hydroponic material (perlite). Third, this investigation provides insight into the suitability of the biosolids and perlite for use as soil amendments.

## Materials and methods

### Sampling sites

Biosolid samples were collected from Nacogdoches Wastewater Treatment Plant (NWWTP), Lufkin Wastewater Treatment Plant (LWWTP), and Angelina-Neches Compost Facility (NCF) (Fig. 1). The Nacogdoches Wastewater Treatment Plant (NWWTP) is located at 2977 Rayburn road, latitude 31° 33' 31.2444" N, longitude 94° 38' 52.1808" W, Nacogdoches, Texas. It has a treatment capacity of 12.88 million gallons per day (MGD) (Onchoke et al., 2018a). Lufkin Wastewater Treatment Plant (LWWTP) is located at 300 E.

Shepherd, latitude 31° 17' 13.8804" N, longitude 94° 44' 56.2416" W, Lufkin, Texas, with a treatment capacity of 11.3 MGD. The Angelina-Neches Compost Facility (NCF) is located at 1805, Highway 79 W, 31°54' 1.552" N, longitude 95°24' 16.451" W, Jacksonville, Texas.

### Materials and chemical reagents

Biosolid samples were collected in plastic containers, air-dried and sieved through a 2.36-mm diameter standard testing sieve (from A.S.T.M, Milwaukee, Wisconsin, U.S.A.). All reagents used were of high analytical purity. All plastic containers and bottles for sampling, storage, and processing were acid-cleaned with conc. nitric and hydrochloric acids (70% ACS reagent (HNO<sub>3</sub>), Flinn Scientific Inc., Batavia, IL, USA). Ultrapure water (18.2 MΩ), HNO<sub>3</sub> and HCl (Flinn Scientific Inc.), hydrogen peroxide (35% wt, Sigma Aldrich), and KBr (Sigma Aldrich Chemical Co.) were used as received. The ICP-OES solutions for metal calibration standards were prepared from 1000 mg/L stock solutions.

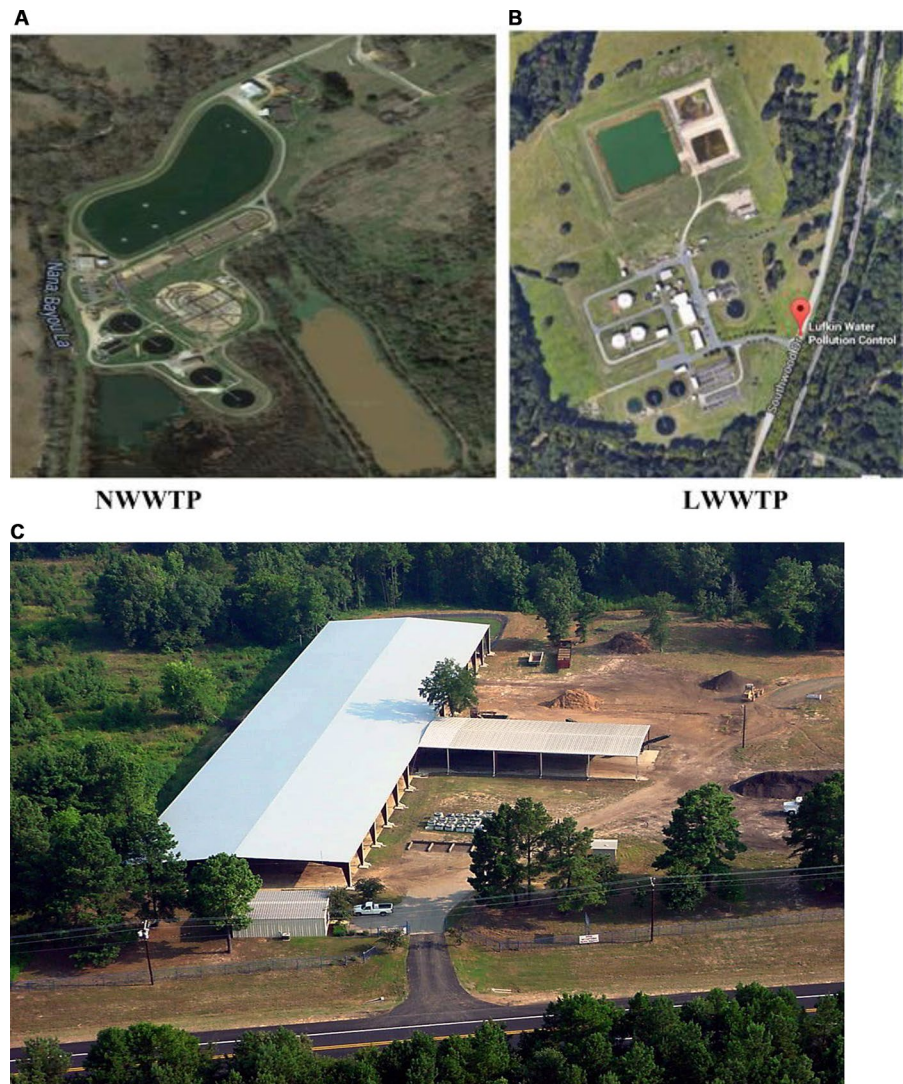
### Physical chemical characterization of biosolids

The pH of biosolids was measured potentiometrically using USEPA methods 9050D and 9050A (APHA, 2013). About 20.0000 g of each sample was mixed with 40 mL ultrapure water (18.2 MΩ). The biosolid-water slurry was suspended for 1 h, and a pH 211 microprocessor (pH meter, HANNA instruments) was used. The electrical conductivity of the biosolid samples was determined with USEPA method 9054A (APHA, 2013). Biosolid-water slurry was made with 50 mL 18.2 MΩ nanopure water and the suspension shaken at 15 rpm for 60 min. The KCl was used to calibrate the meter prior to measuring the conductivity of the soil-water suspension (APHA, 2013).

### Digestion of samples prior to analysis with ICP-OES

The total metal content in biosolids and perlite was determined via digestion procedures described in USEPA method 3050B (USEPA, 1996) and in Ref. # (Onchoke et al., 2018a). Approximately 0.5000 g of each air-dried soil therapy compost (STC), perlite (PER), Nacogdoches wastewater sludge (NWS), Lufkin wastewater sludge (LWS), and CRM (Certified Reference Material, SCP Science, [www.scpscience.com](http://www.scpscience.com), Graham, NY) samples were weighed in quadruplicates in Digitubes, and digestions performed using 1:1 HNO<sub>3</sub> (70% (v/v), ACS

**Fig. 1** Aerial view of Nacogdoches (A, NWWTP), Lufkin Waste-water Treatment Plant (B LWWTP), and Angelina-Neches Compost Facility (C, NCF). A and B are adopted from Ref (Onchoko et al., 2018a)



reagent, Flinn Scientific Inc, Batavia, IL, USA) and  $\text{H}_2\text{O}_2$  (35% (w/w), Sigma Aldrich, St. Louis, MO). A digestion block (SCP Science, [www.scpscience.com](http://www.scpscience.com), Graham, NY) was used to reflux the biosolid samples, which were thereafter filtered with a  $0.45\text{-}\mu\text{m}$  filter. Standard solutions and dilutions of filtered biosolid samples were prepared in  $18.2\text{ M}\Omega\cdot\text{cm}$  water.

Spectroscopic characterization of samples

*Inductively coupled plasma-optical emission spectroscopy (ICP-OES)*

An Agilent ICAP 7400 ICP-OES (dual view, ThermoScientific) was used to analyze the total metal

content in biosolid samples. The detailed information for determination of metal concentrations is presented in “[Digestion of samples prior to analysis with ICP-OES](#)” section.

*Fourier transform infrared spectroscopy (FT-IR)*

Air-dried samples were finely ground with agate mortar and pestle and loaded onto a silicon abrasive pad. Infrared spectra were then recorded with the use of diffuse reflectance infrared Fourier transform spectroscopy (DRIFTS) with Perkin-Elmer Spectrum100 spectrometer in the spectral region  $230\text{--}4000\text{ cm}^{-1}$  at  $4\text{ cm}^{-1}$  resolution. Up to 300 scans were acquired.



### SEM/EDX analysis

The surface morphology, structure, and elemental composition of samples were determined using a JEOL-JSM-6100 scanning electron microscope equipped with a Horiba energy-dispersive X-ray spectroscopy (EDX). The electron microscope was operated at an accelerated voltage of 20 KV and filament current of 200 A. To lower electron charging, an Automatic Platinum Sputter Coater System (Quorum Q150RS) was used to coat biosolid samples with Pd/Au.

### Powder X-ray diffraction (XRD) spectroscopy

The crystalline phases and composition of samples were determined by using powder XRD. A Bruker AXS D8 Advance diffractometer equipped with an X-ray tube (Cu K $\alpha$  radiation:  $\lambda = 1.54060 \text{ \AA}$ , 40 kV, and 40 mA) was used with a Ni filter and one-dimensional LynxEye detector at scanning speeds of 2°/min and step sizes of 0.0125° and 1s/step. Procedures reported in Ref. (Onchoke et al., 2018a) were adopted and followed for line fitting.

### Thermogravimetric analysis (TGA) of samples

Thermogravimetric analysis of biosolids was performed in a thermogravimetric simultaneous thermal analyzer (STA 6000, Perkin-Elmer TGA/DTA) under a N<sub>2</sub> atmosphere. About 20.0 mg of samples was used for each analysis at 10 °C/min, 20 °C/min, 30 °C/min, and 40 °C/min heating rates in the range 30–1000 °C.

### Quality control and quality assurance

Method validation was carried out by comparing ICP-OES and certified values for Certified Reference Material (CRM, EnviroMAT SS-2, SCP Science, [www.scpscience.com](http://www.scpscience.com), Clark Graham, Canada). Table 1 shows percent agreement between measured values and the Certified Reference Material. The approximate percent agreement of 80 to 120% between the measured and CRM values were considered useful for analysis. The limit of detection (in ppm) for each element analyzed are given as follows: Ag/0.00187, Al/0.00281, As/0.00815, B/0.0257, Ba/0.000469, Ca/0.503, Cd/0.000407 (@  $\lambda = 228.802 \text{ nm}$ ), Cd/0.000391 (@  $\lambda = 226.502 \text{ nm}$ ), Co/0.000473, Cr/0.00126, Cu/0.00426,

Fe/0.00260, Hg/0.00255, K/0.236, Mg/0.00870, Mn/0.0002, Mo/0.000408, Na/0.844, Ni/0.00151, P/0.00685, Pb/0.00666, S/0.00829, Se/0.0145, V/0.00163, and Zn/0.000322 (in alphabetical order).

## Results and discussion

### Physical chemical characterization of biosolids

The measured pH of biosolids and perlite samples (Table 2) varied in the range 5.32 to 6.77, in ascending order: NWWS ( $5.33 \pm 0.01$ ) < LWWS ( $5.78 \pm 0.01$ ) < STC ( $6.74 \pm 0.03$ ). The measured pH is comparable to other reports for biosolids in the range  $6.01 \pm 0.26$  and 5.84–8.12 (Kengne et al., 2009; Tandy et al., 2009). Plants thrive well in the soil pH range 5.50–7.50 (Rengel, 2002). Thus, all samples are suitable as soil media for plant growth. The physicochemical properties of the sludge used in this work are similar to previously reported work from Nacogdoches and Lufkin wastewater treatment plants (NWWTP, LWWTWP) as listed in Table 2 (Onchoke et al., 2018a).

### Spectroscopic analysis of biosolids and perlite

#### Determination of metal concentrations in Biosolids via ICP-OES

**Macroelements** Figure 2a, b and Table 3 depict macroelement concentrations in STC, NWWS, LWWS, and perlite (PER) samples. Notably, essential nutrients P and K necessary for plant growth are present in samples. Except for Fe (LWWS ( $15163 \pm 2212 \text{ ppm}$ ), NWWS ( $32890 \pm 2695 \text{ ppm}$ )), concentrations of other elements were relatively similar in LWWS and NWWS. Comparatively, perlite (PER, Fig. 2b) contained low amounts of macroelements (Al ( $1176 \pm 322 \text{ ppm}$ ), Ca ( $3632 \pm 1035 \text{ ppm}$ ), Fe ( $1338 \pm 248 \text{ ppm}$ ), K ( $9337 \pm 1281 \text{ ppm}$ ), Mg ( $654 \pm 236 \text{ ppm}$ ), P ( $4649 \pm 790 \text{ ppm}$ ), S ( $2097 \pm 227 \text{ ppm}$ ), Na ( $195 \pm 1658 \text{ ppm}$ )). The order of concentrations of macro-elements in biosolids and perlite follow the trend: NWWS (Al ( $15591 \pm 1692 \text{ ppm}$ ), Fe ( $32890 \pm 2695 \text{ ppm}$ ), Mg ( $7293 \pm 647 \text{ ppm}$ ), P ( $26102 \pm 1522 \text{ ppm}$ )); LWWS (Al ( $12217 \pm 1985 \text{ ppm}$ ), Fe ( $15163 \pm 2212 \text{ ppm}$ ), Mg ( $4116 \pm 561 \text{ ppm}$ ), P ( $20855 \pm 2594$ )); STC (Al ( $12424 \pm 824 \text{ ppm}$ ), Fe ( $13352 \pm$

**Table 1** ICP-OES analysis of certified reference material (CRM), (SCP Science, SS-2, EnvironMAT) the standard deviations, (mean  $\pm$  concentration), and the approximate percent agreement (*Bd* below detection)

Element	Number of reference samples ( <i>n</i> )	CRM SS-2 (reference consensus value) (mean), ppm	Measured (Mean $\pm$ SD), ppm	Approximate percent agreement
Ag	4	1.3 $\pm$ n/a (no confidence interval)	Bd	-
Al	4	13265 $\pm$ 1151	15102 $\pm$ 275	113.85
As	4	75 $\pm$ 10	88.0 $\pm$ 2.87	117.33
B	4	12 $\pm$ n/a (no confidence interval)	11.6 $\pm$ 0.39	96.67
Ba	4	215 $\pm$ 13	244.4 $\pm$ 5.2	104.6
Ca	4	112861 $\pm$ 4872	121381 $\pm$ 2658	107.55
Cd	4	2 $\pm$ n/a (no confidence interval)	1.7 $\pm$ 0.1	86.50
Co	4	12 $\pm$ 1	12.69 $\pm$ 0.12	97.61–105.75
Cr	4	34 $\pm$ 4	39.5 $\pm$ 0.77	103.9–116.76
Cu	4	191 $\pm$ 9	213 $\pm$ 6	111.52
Fe	4	21046 $\pm$ 1449	22524 $\pm$ 174	107.02
Hg	4	0.28 $\pm$ n/a (no confidence interval)	Bd	-
K	4	3418 $\pm$ 351	4619.65 $\pm$ 1189.55	135.16
Mg	4	11065 $\pm$ 606	12208 $\pm$ 166	110.33
Mn	4	457 $\pm$ 24	521.4 $\pm$ 7.52	114.09
Mo	4	4 $\pm$ n/a (no confidence interval)	2.4 $\pm$ 0.22	60
Ni	4	54 $\pm$ 4	54.51 $\pm$ 1.69	100.94
P	4	734–770	1022 $\pm$ 36	134.3
Pb	4	126 $\pm$ 10 (116–136)	131.5 $\pm$ 1.09	104.37
S	4	2193 $\pm$ n/a (no confidence interval)	3544.66 $\pm$ 33.66	161.64
Se	4	0.8 (no confidence interval)	Bd	-
Zn	5	467 $\pm$ 23	484.18 $\pm$ 5.21	103.67
V	4	34 $\pm$ 3	40.30 $\pm$ 0.91	118.53
Na	4	558 $\pm$ 102	783.00 $\pm$ 21.36	118.64–140.32

**Table 2** Analysis of physico-chemical properties of air-dried sewage sludge (*n* = 3)

Analyte	Results (mg kg <sup>-1</sup> )			
	NWWTS	LWWTS	STC	Perlite
pH	5.33 $\pm$ 0.01 <sup>a</sup>	5.78 $\pm$ 0.01 <sup>a</sup>	6.74 $\pm$ 0.03 <sup>b</sup>	5.77 $\pm$ 0.03 <sup>b</sup>
	5.87 $\pm$ 0.03 <sup>b</sup>	6.99 $\pm$ 0.09 <sup>b</sup>		
C (%)	32.5 $\pm$ 0.02	30.9 $\pm$ 0.01	33.70 <sup>c</sup>	ND
N (%)	9.8 $\pm$ 0.7	8.4 $\pm$ 0.8	1.59	ND
P	935 $\pm$ 20	1705 $\pm$ 30	6600 <sup>c</sup>	4649 $\pm$ 790
S	211	1478	-	2097 $\pm$ 227
Total Ca	1521	3869	4200 <sup>c</sup>	3632 $\pm$ 1035
Total Mg	574	709	700 <sup>c</sup>	654 $\pm$ 236
Total K	675	679	700 <sup>c</sup>	9337 $\pm$ 1281
Organic matter (mg/kg)	64.9	61.8	67.40	ND
NH <sub>4</sub> <sup>+</sup> -N (mg/kg)	170	205	ND	ND

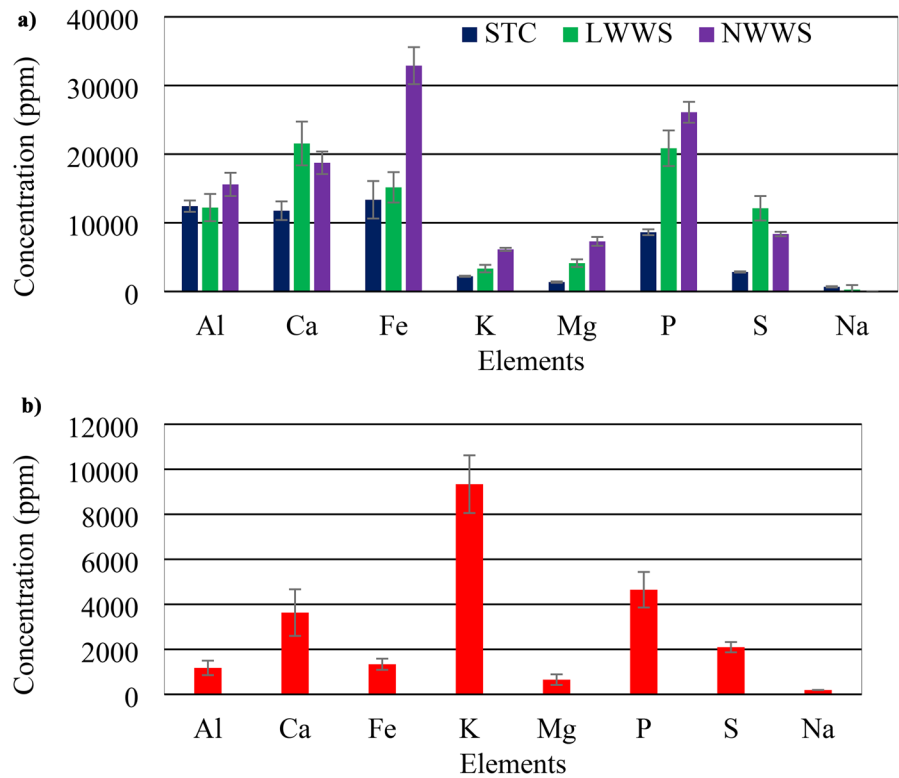
Where no standard deviation is given, only one sample measurement was made once

ND not determined

<sup>a</sup>Reported in Ref # (Onchoke et al., 2018a)

<sup>b</sup>this study

**Fig. 2** Macroelement concentrations (ppm) of (a) STC ( $n = 4$ ), LWWS, NWWS ( $n = 3$ ), and perlite (b,  $n = 4$ ). Standard deviations are shown in the graph



2731 ppm), Mg ( $1362 \pm 98$  ppm), P ( $8623 \pm 426$  ppm)) > PER (Al ( $1176 \pm 322$  ppm), Fe ( $1338 \pm 248$  ppm), Mg ( $645 \pm 236$  ppm), P ( $4649 \pm 790$  ppm)), for Ca: LWWS ( $21552 \pm 3186$  ppm) > NWWS ( $18738 \pm 1644$  ppm) > STC ( $11760 \pm 1358$  ppm) > PER ( $3632 \pm 1035$  ppm), and K: PER ( $9337 \pm 1281$  ppm) > NWWS ( $6126 \pm 229$  ppm) > LWWS ( $3328 \pm 548$  ppm) > STC ( $2207 \pm 82$  ppm).

**Microelements** Figure 3a, b and Table 2 depict the concentrations of microelements in STC, NWWS, LWWS, and PER. Notably, Ba, Cu, Zn, and Mn are observed in higher concentrations in all samples. The microelements Ba (LWWS –  $319 \pm 44$  ppm, NWWS –  $563 \pm 45$  ppm, STC –  $308 \pm 14$  ppm), Cu (LWWS –  $531 \pm 78$  ppm, NWWS –  $386 \pm 35$  ppm, STC –  $338 \pm 14$  ppm), Mn (LWWS –  $1262 \pm 192$  ppm, NWWS –  $1136 \pm 102$  ppm, STC –  $794 \pm 39$  ppm) and Zn (LWWS –  $883 \pm 127$  ppm, NWWS –  $810 \pm 71$  ppm, STC –  $409 \pm 14$  ppm) were present in higher concentrations vis-a-vis other microelements. Microelements concentrations occur in the order Ba: NWWS ( $563 \pm 45$  ppm) > LWWS ( $319 \pm 44$  ppm) > STC ( $308 \pm 14$  ppm) > PER ( $31 \pm 7.2$  ppm), Cu, Mn, Zn:

LWWS (Cu ( $531 \pm 78$  ppm), Mn ( $1262 \pm 192$  ppm), Zn ( $883 \pm 127$  ppm)) > NWWS (Cu ( $386 \pm 35$  ppm), Mn ( $1136 \pm 102$  ppm), Zn ( $810 \pm 71$  ppm)) > STC (Cu ( $338 \pm 14$  ppm), Mn ( $794 \pm 39$  ppm), Zn ( $409 \pm 14$  ppm)) > PER (Cu ( $2 \pm 0.6$  ppm), Mn ( $27 \pm 6$  ppm), Zn ( $10 \pm 2$  ppm)). Figure 3a shows that toxic elements As, Cd, Cr, Hg, Co, and Pb were detectable in concentrations < 30 ppm. The regulated microelements As, Cd, Cr, Cu, Hg, Pb, Mo, Ni, and Zn were found below USEPA maximum concentration limits (Table 3), consistent with previous reported findings (Onchoke et al., 2018a).

**FTIR analysis of biosolids** Figure 4a–c compare infrared spectra of NWWS, LWWS, and STC in the  $240\text{--}4000\text{ cm}^{-1}$  region, respectively. As observed, no significant differences are noted in band and peak positions. This suggests similarity of functional groups. The broad band at  $3600\text{--}3200\text{ cm}^{-1}$  indicates the presence of an -O-H or N-H stretching of carboxyl, phenolics or amino groups. Bands at  $3000\text{--}2700\text{ cm}^{-1}$  and  $1640\text{ cm}^{-1}$  are ascribed to  $\text{sp}^3$  C-H stretching, and carbonyl and amide groups, respectively. The peaks in the  $1250\text{--}1000\text{ cm}^{-1}$  region

**Table 3** Mean  $\pm$  standard deviation of metals in the biosolid samples analyzed with ICP-OES and their corresponding USEPA limit

Element	Samples				USEPA ceiling limit (ppm)
	STC (ppm) ( $n = 4$ )	PER (ppm) ( $n = 4$ )	LWWS (ppm) ( $n = 3$ )	NWWS (ppm) ( $n = 3$ )	
Ag	1.11 $\pm$ 0.30	Bd	Bd	0.58 $\pm$ 0.38	-
Al	12424 $\pm$ 824.48	1175.90 $\pm$ 321.63	12217 $\pm$ 1985	15591 $\pm$ 1692	-
As	5.48 $\pm$ 0.62	2.77 $\pm$ 0.81	20.09 $\pm$ 2.79	11.68 $\pm$ 0.64	75
B	Bd	Bd	Bd	107.2 $\pm$ 20.63	-
Ba	308.16 $\pm$ 13.64	30.84 $\pm$ 7.17	318.56 $\pm$ 44.25	563 $\pm$ 45.29	-
Ca	11760 $\pm$ 1358.16	3632 $\pm$ 1035.31	21552 $\pm$ 3186	18738 $\pm$ 1644	-
Cd	0.19 $\pm$ 0.07	0.05 $\pm$ 0.03	0.20 $\pm$ 0.03	Bd	85
Cr	4.25 $\pm$ 0.18	0.93 $\pm$ 0.36	11.08 $\pm$ 1.67	16.70 $\pm$ 1.71	3000
Co	14.35 $\pm$ 0.38	4.85 $\pm$ 1.75	24.69 $\pm$ 3.76	25.74 $\pm$ 3.48	-
Cu	337.51 $\pm$ 14.35	1.98 $\pm$ 0.58	530.91 $\pm$ 78.26	386.4 $\pm$ 34.86	4300
Fe	13352 $\pm$ 2731	1338 $\pm$ 248.40	15163 $\pm$ 2212	32890 $\pm$ 2695	-
Hg	Bd	Bd	Bd	Bd	57
K	2206.96 $\pm$ 81.59	9337.2 $\pm$ 1281.49	3328 $\pm$ 547.95	6126 $\pm$ 229.44	-
Mg	1362.43 $\pm$ 97.71	654.09 $\pm$ 236.114	4116 $\pm$ 561.34	7293 $\pm$ 646.98	-
Mn	793.62 $\pm$ 38.56	26.77 $\pm$ 5.73	12623 $\pm$ 191.73	1136 $\pm$ 101.86	-
Mo	3.90 $\pm$ 0.87	Bd	7.67 $\pm$ 1.32	7.29 $\pm$ 0.72	75
Ni	17.49 $\pm$ 0.38	9.08 $\pm$ 1.29	33.46 $\pm$ 1.21	44.04 $\pm$ 4.21	420
P	8623.35 $\pm$ 425.64	4649.08 $\pm$ 789.97	20855 $\pm$ 2594	26102 $\pm$ 1522	-
Pb	16.99 $\pm$ 0.57	Bd	29.21 $\pm$ 3.44	26.51 $\pm$ 0.59	840
S	2837.95 $\pm$ 89.21	2096.93 $\pm$ 227.26	12116 $\pm$ 1784	8365 $\pm$ 330.67	-
Se	Bd	Bd	Bd	Bd	100
Zn	408.58 $\pm$ 13.98	10.06 $\pm$ 1.98	882.53 $\pm$ 127.42	810.36 $\pm$ 71	7500
V	12.13 $\pm$ 2.25	5.37 $\pm$ 1.06	7.80 $\pm$ 1.31	33.26 $\pm$ 3.27	-
Na	668.31 $\pm$ 91.96	194.45 $\pm$ 1658.34	271.49 $\pm$ 658.58	Bd	-

( $n = 4$  for STC (soil therapy compost),  $n = 3$  for NWWS (Nacogdoches wastewater sludge),  $n = 3$  for LWWS (Lufkin wastewater sludge),  $n = 4$  for PER (perlite), *Bd* below detection)

indicate a C-N group. The peaks at 1375  $\text{cm}^{-1}$ , 695  $\text{cm}^{-1}$ , and 563  $\text{cm}^{-1}$  are ascribed to the presence of C-F, C-Cl, and C-Br, respectively (Socrates, 1994). The presence of the O-H group and the C=O at 1640  $\text{cm}^{-1}$  strongly indicates the presence of carboxylic acids. The peaks around 1000  $\text{cm}^{-1}$  are attributable to Si-O stretching suggesting the presence of quartz, as evident from XRD studies (Onchoke et al., 2018a).

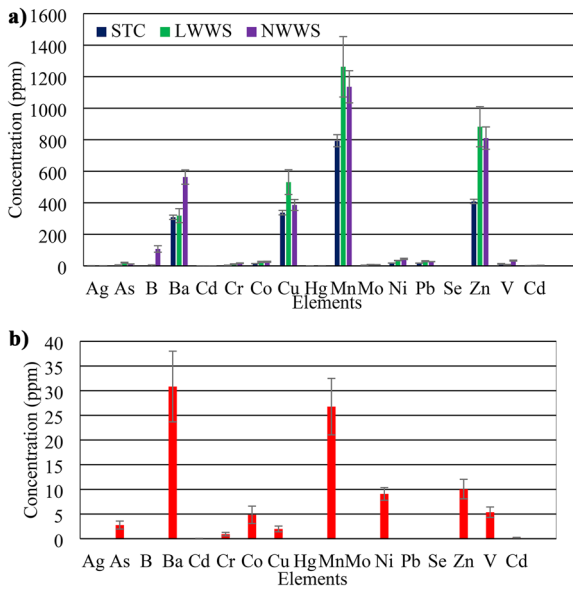
#### Elemental composition of biosolids with SEM/EDX

Figure 5a–d (and Supplementary Fig. S1) depict the SEM micrographs for STC, NWWS, and LWWS, and perlite, respectively. The particle size diameters are observed in the range 25–350  $\mu\text{m}$ , in agreement

with results which showed particle diameters in the range 1–500  $\mu\text{m}$  (Choo & Lee, 1998; Onchoke et al., 2018c). Notably, sludges are porous materials with average diameter size of about 20–50  $\mu\text{m}$  with features in the nanometer scale (Onchoke et al., 2018a). Cheng et al. (2016) measured large particle sizes in hundreds of micrometers. This property renders biosolids advantageous for use in separations.

Figure 6a–c show the EDX graphs along with respective elemental compositions of STC, NWWS, and LWWS. The elemental composition shows macroelements Al, Ca, Fe, K, P, and S, which were detected with ICP-OES. These elements occur in approximate equivalent amounts in NWW, LWWS, and STC biosolids. Due to low detection limits by EDX,





**Fig. 3** Microelement concentrations (ppm) of (a) STC ( $n = 4$ ), LWWS, NWWS ( $n = 3$ ), and perlite (b,  $n = 4$ ). Standard deviations are shown in graph

elements As, Cd, Hg, and Pb were below detection vis-a-vis C, O, Sc, Cl, and Si. In decreasing trend, elemental % wt/wt concentrations in STC occur in the order O (39.8) > C (34.3 %) > Si (9.1 %) > Al (1.7 %) > Na (0.7 %) > P (0.6 %) > Ca (0.5 %) > S (0.2 %). The order of % wt/wt concentration of elements in decreasing trend in NWWS was O (45.8 %) > C (41.5 %) > Si (3.8 %) > Fe (2.9 %) > P (2.0 %) > Al (1.4 %) > Mg (0.7 %) > Na (0.6 %)  $\approx$  Ca (0.6 %) > Co (0.0 %).

*X-ray powder diffraction patterns (XRD) of biosolids*

Figure 7a, b, and b show the X-ray powder diffraction pattern of NWWS, LWWS and STC, respectively. The sharp peaks show the crystalline nature of biosolids and composted sludge. Notably, the comparable XRD patterns are similar in peak positions. These results imply similarity in the sources of the components of the materials. The literature shows that the  $2\theta$  and d-spacing values ( $6.070^\circ$ , 14.55), ( $20.58^\circ$ , 4.55), and ( $26.40^\circ$ , 3.36) are attributed to the presence of vermiculite ( $\text{CaSO}_4 \cdot 2\text{H}_2\text{O}$ ), alunogen ( $\text{Al}_2(\text{SO}_4) \cdot 17\text{H}_2\text{O}$ ), and quartz ( $\text{SiO}_2$ ), respectively (Onchoke et al., 2018a). Other crystalline phases include vermiculite ( $d = 31.21^\circ$ , 2.29;  $30.26^\circ$ , 2.47),

gypsum ( $20.68^\circ$ , 4.31), parygoskite ( $40.03^\circ$ , 2.14), and hexahydrate ( $45.51^\circ$ , 1.99) (Fig. 7).

*Thermogravimetric analysis (TGA) and derivative TGA (DTGA)*

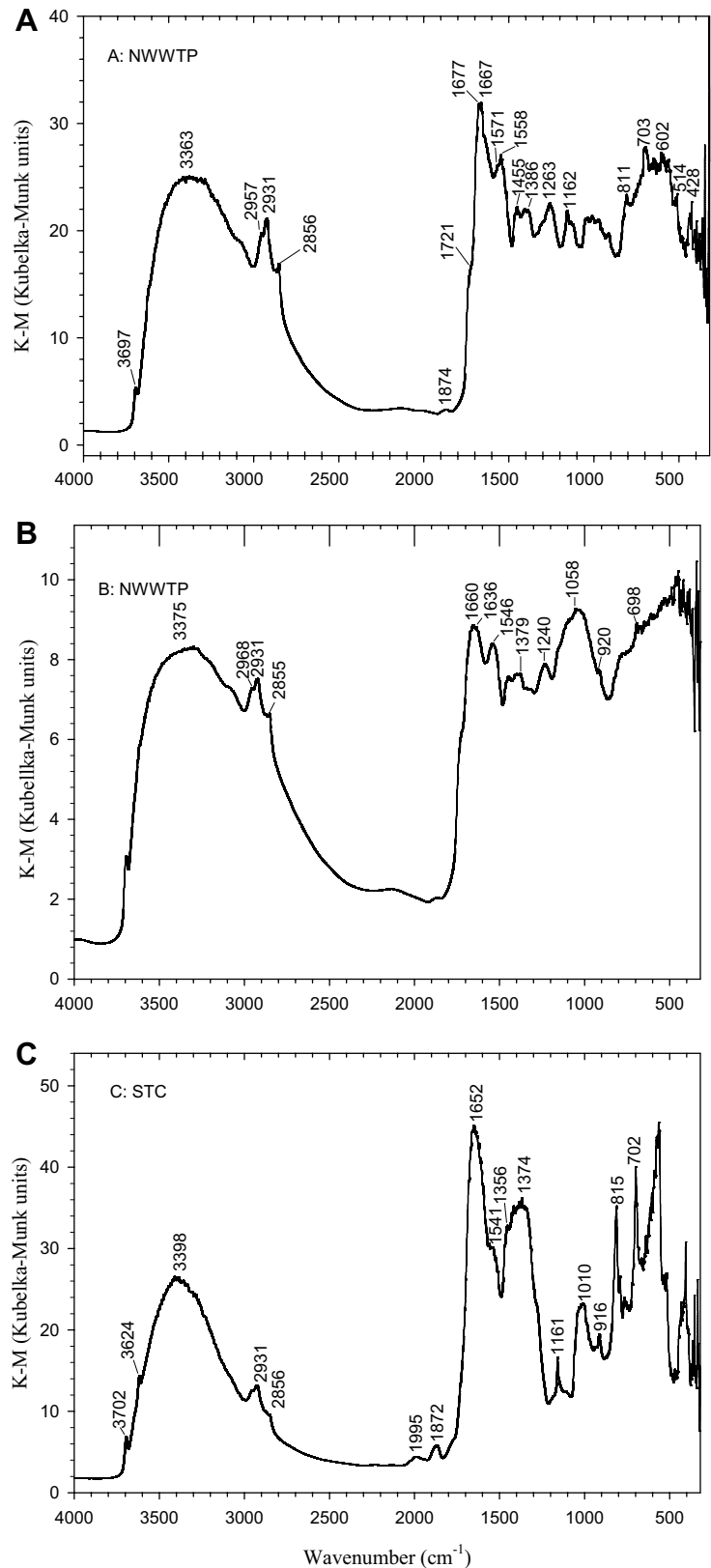
Figure 8 (panels I and II) and S2 (Supplementary Information Fig. S2) show the phase changes that occur upon decomposition of biosolid samples heated at  $10^\circ\text{C}/\text{min}$ ,  $20^\circ\text{C}/\text{min}$ ,  $30^\circ\text{C}/\text{min}$ , and  $40^\circ\text{C}/\text{min}$  in the range 30 to  $1000^\circ\text{C}$ . The TGA and DTGA thermograms (Fig. 8, panels I and II, and Fig. S2) can be subdivided into four decomposition stages, namely,  $33\text{--}110^\circ\text{C}$ ,  $110\text{--}220^\circ\text{C}$ ,  $220\text{--}400^\circ\text{C}$ , and  $400\text{--}800^\circ\text{C}$ . The initial stage at  $33\text{--}110^\circ\text{C}$  is attributed to loss of moisture content (Tettamanti et al., 2001). The second stage occurring at  $220\text{--}400^\circ\text{C}$  indicates the breakdown of small volatile compounds with weak hydroxyl bonds (Li et al., 2015). The final stage at  $400\text{--}800^\circ\text{C}$  are attributable to loss of inorganic compounds  $\text{SiO}_2$ ,  $\text{Al}_2\text{O}_3$ ,  $\text{MgO}$ ,  $\text{Fe}_2\text{O}_3$ , and  $\text{CaO}_3$  (Magdziarz & Wilk, 2013). Figure 8 shows that the biosolids' TGA curves are similar at the four heating rates. The first, second, third, and fourth stages (Fig. S2) show approximate weight losses of 5–9.8%, 6–8.5%, 10.92%, and 7.04%, respectively.

*Spectroscopic and thermogravimetric implications of current study*

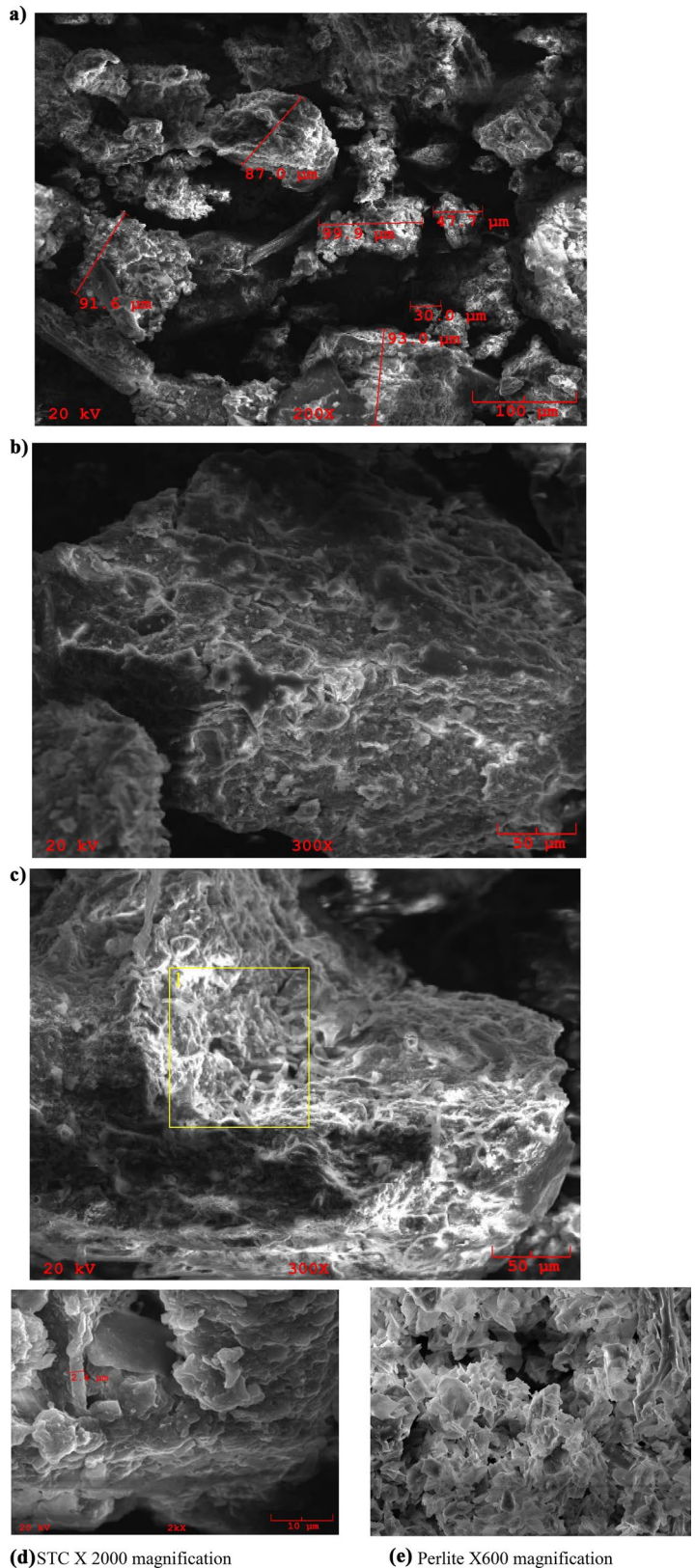
This study assessed the nutrients available for plant growth and yield, and thus enhances understanding of the suitability and/or application rates to agricultural fields, and possible pollutant levels in biosolids. In this study, the pH, a critical parameter that controls the uptake of metals by plants, especially when present in the labile form, varied in the range 5.33–6.74, indicating favorable pH of biosolids at which plants thrive between 5.2 and 7.3 (Mtshali et al., 2014; Smernik et al., 2003). Experiments show that more plant nutrients are available at pH of about 6 (McConnell et al., 1993). This therefore makes the NWWS, LWWS, and STC biosolids suitable for land application.

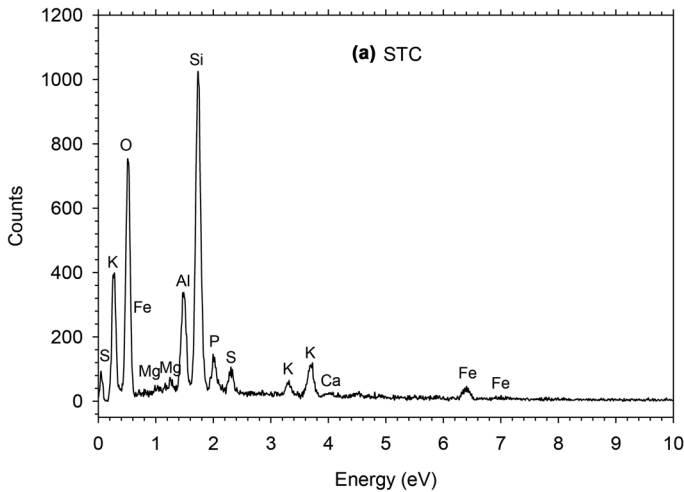
Analysis of biosolids via ICP-OES yields information on the concentrations of macro- and microelements in the biosolids. Microelements (Mn, Zn, Fe, Cu, Mo, Ni) essential for plant growth were determined present in the biosolids. Heavy metals As ( $\text{STC-}5.48 \pm$

**Fig. 4** FT-IR (DRIFTS) spectra of biosolids NWS, LWS and STC from NWWTP (A), LWWTP (B), and NCF (C), respectively, acquired at  $4\text{ cm}^{-1}$  resolution

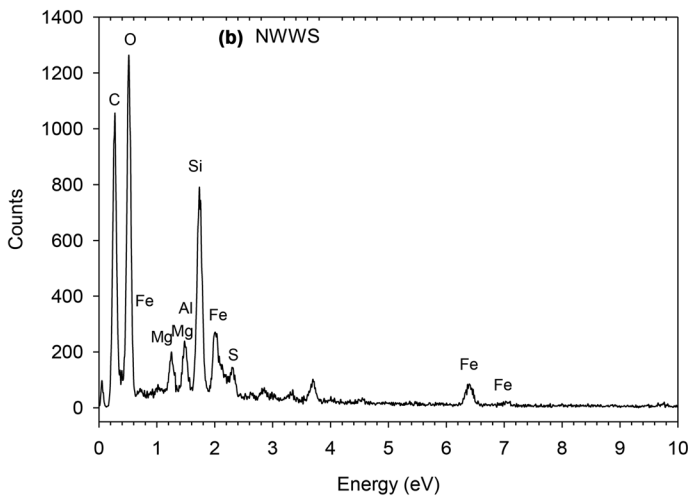


**Fig. 5** SEM micrograph for STC (a), NWWS (b), and LWWS (c) at a  $\times 300$  magnification, an accelerated voltage of 20 KV, and filament current of 200 A. The SEM micrographs for STC (d), and perlite (e) at  $\times 600$  magnification, were acquired with the following parameters: an accelerated voltage of 20 KV, and filament current of 200 A

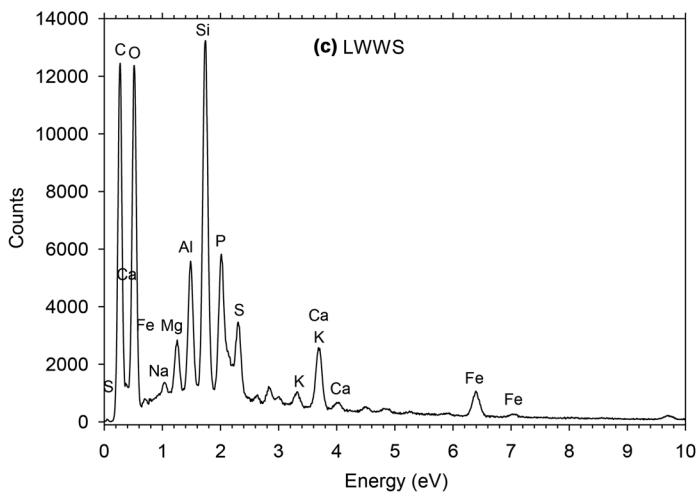




Elt.	Line	Intensity (c/s)	Atomic %	Conc. (wt %)
O	K $\alpha$	110	70	56.0
Mg	K $\alpha$	3.5	0.5	0.6
Al	K $\alpha$	50	5.5	7.4
Si	K $\alpha$	168	17	24.3
P	K $\alpha$	16	1.9	2.9
S	K $\alpha$	12	1.2	1.9
K	K $\alpha$	7.2	0.6	1.2
Ca	K $\alpha$	21	1.7	3.4
Fe	K $\alpha$	8.0	0.9	2.4
			100.0	100.0



Elt.	Intensity (c/s)	Atomic %	Conc (wt %)
C	135	48	38.5
O	171	45	47.6
Mg	19	0.8	1.3
Al	25	0.8	1.4
Si	121	3.2	6.0
P	44	1.1	2.3
S	18	0.4	0.9
Fe	18	0.5	2.0
		100.0	100.0



Elt.	Line	Intensity (c/s)	Atomic %	Conc (wt %)
C	K $\alpha$	2,262	52	41
O	K $\alpha$	2,299	39	41
Na	K $\alpha$	110	0.4	0.6
Mg	K $\alpha$	256	0.6	0.9
Al	K $\alpha$	794	1.4	2.4
Si	K $\alpha$	2,497	3.7	6.8
P	K $\alpha$	995	1.5	3.0
S	K $\alpha$	509	0.7	1.4
K	K $\alpha$	104	0.1	0.3
Ca	K $\alpha$	458	0.5	1.4
Fe	K $\alpha$	213	0.4	1.3
			100.0	100.0

◀**Fig. 6** EDX elemental composition of soil therapy compost (STC) (a), Nacogdoches wastewater sludge (NWWS) (b), and Lufkin wastewater sludge (LWWS) (c). EDX was acquired at a magnification of X300, an accelerated voltage of 20 KV, and filament current of 200 A. The percentage composition (% wt/wt) of elements in each of the wastewater sludge (WWS) is shown alongside each spectrum

0.62 ppm, LWWS- $20 \pm 2.79$  ppm, NWWS- $12 \pm 0.64$  ppm), Cd (STC- $0.19 \pm 0.07$  ppm, LWWS- $0.20 \pm 0.03$  ppm, NWWS-Below detection), Cr (STC- $4.3 \pm 0.18$  ppm, LWWS- $0.93 \pm 1.67$  ppm, NWWS- $17 \pm 1.71$  ppm), and Pb (STC- $17 \pm 0.57$  ppm, LWWS- $29 \pm 3.44$  ppm, NWWS- $27 \pm 0.59$  ppm) in the biosolid samples were found below USEPA ceiling limits (Table 3). This is in accordance with studies that found low metal concentrations in biosolids vi-a-vis USEPA regulatory limits (Islam et al., 2013; Onchoke et al., 2018a; Urasa & Macha, 1999; Westerhoff et al., 2015; Yang et al., 2014). Although metal concentration results in this study suggest a reasonable recommendation for land application, continued use over long periods portends risk of accumulation in soils.

The FTIR spectra for biosolids exhibited absorption peaks indicative of functional groups -OH, C-H, C=O, and C-N (Socrates, 1994) in agreement with previous studies by Zhou et al. (2000) and Onchoke et al. (2018a). In addition, FTIR peaks revealed the presence of functional groups C-F, C-Cl, and C-Br (Socrates, 1994). The presence of functional groups -COOH and -OH in biosolids causes complexation of heavy metals in biosolids. This can lead to enhanced solubility and mobility of heavy metals in biosolids and thus result in increased uptake of metals by plants (Al-Wabel et al., 2002; Han & Thompson, 1999). On a microscopic level, the SEM/EDX micrograph shows biosolid particle diameters in 25–50  $\mu\text{m}$  range. This suggests that biosolids are micron-sized materials, in agreement with previous studies (Kiser et al., 2009; Onchoke et al., 2018a; Onchoke et al., 2018c). The multi-pronged spectroscopic analyses are therefore significant in establishing the presence of both regulated and unregulated USEPA metals in sewage sludge. The elemental composition determined with EDX further confirms the presence of detected elements Al, Ca, K, P, Cu, Zn, and Cd by using ICP-OES (Fig. 3).

The presence of vermiculite ( $\text{CaSO}_4 \cdot 2\text{H}_2\text{O}$ ), alunogen ( $\text{Al}_2(\text{SO}_4) \cdot 17\text{H}_2\text{O}$ ), and quartz ( $\text{SiO}_2$ ) with d-spacings 14.55, 4.55, and 3.36, respectively, in biosolid samples, was in agreement with other studies (Ling et al., 2017

; Vemic et al., 2015). Ling et al. (2017) found a peak with a  $2\theta$  and d-spacing values for quartz at  $26.641^\circ$  and 3.346. A peak observed for vermiculite and alunogen exhibited similar  $2\theta$  and d-spacing as previously reported (Onchoke et al., 2018a).

The TGA and DTGA curves show the presence of volatile organic compounds with weak hydroxyl bonds (Barneto et al., 2009) and inorganic species  $\text{SiO}_2$ ,  $\text{Al}_2\text{O}_3$ ,  $\text{MgO}$ ,  $\text{Fe}_2\text{O}_3$ , and  $\text{CaO}_3$  (Magdziarz & Wilk, 2013). The micrometer/nanoparticles in biosolids can affect the release and mobility of essential nutrients for plant growth from the organic matter fraction. The nanoparticles and microparticles are known to disrupt the plant-microbe relationship that enhance soil fertility (Fayiga & Saha, 2017). Thus, further investigations are recommended.

Notably, NWWS and LWWS are produced from activated wastewater treatment plants and undergo similar treatment processes. It is therefore plausible that NWWS and LWWS contain similar element concentrations and content. However, NCF composted sludge contains lower metal concentrations vis-à-vis regulated USEPA ceiling concentrations. The microcrystalline nature of the biosolids is important to the sequestration of nanomaterials in their crystalline structures.

#### Implications for monitoring and risk assessment in the studied region

The increase in human population necessitates the need to seek innovative monitoring and assessment disposal methods that minimize adverse impacts to the environment. It is evident from this study that determination of metal concentrations is important and central to understanding the bioavailabilities and speciation in various matrices. Furthermore, the SEM morphologies show that biosolid particle sizes occur in the micrometer and/or nanometer regimes, in agreement with previous studies (Onchoke et al., 2018a). To the best of our knowledge, only a few such studies in Texas have been investigated (Onchoke et al., 2018a; Onchoke et al., 2018b; Yang et al., 2014). It is suggested that other analytical technical techniques, including TEM, and single-particle inductively plasma mass spectroscopy (SP-ICP-MS) (Tou et al., 2017) be employed for determination, quantitation, and distribution of nanoparticles (NPs) such as Fe-NPs, Ag,  $\text{TiO}_2$ , zinc oxides/sulfides, titanium



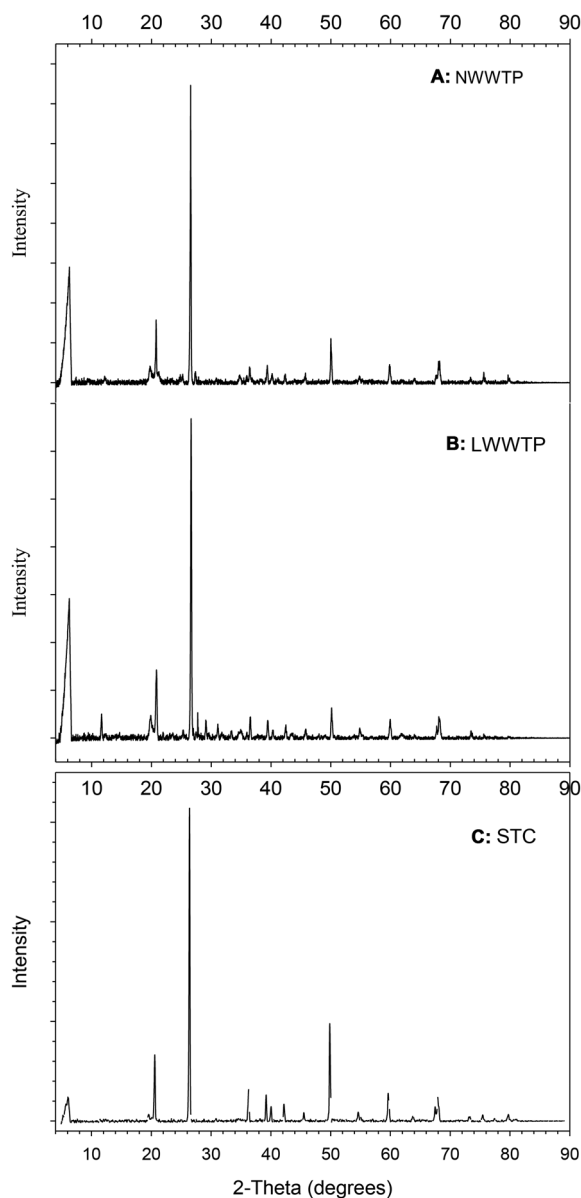


**Fig. 7** Diffractogram XRD patterns for: (a) Nacogdoches and (b) Lufkin wastewater sludge (Onchoke et al., 2018a). The assignment of peaks is given in Ref. # (Onchoke et al., 2018a) and is similar to that of soil therapy compost in c (d-spacing, and h, k, l values of soil therapy compost (STC))

oxides, and CuO, among others (Chen et al., 2015) in complex environmental samples. Investigation of various NPs is thus recommended.

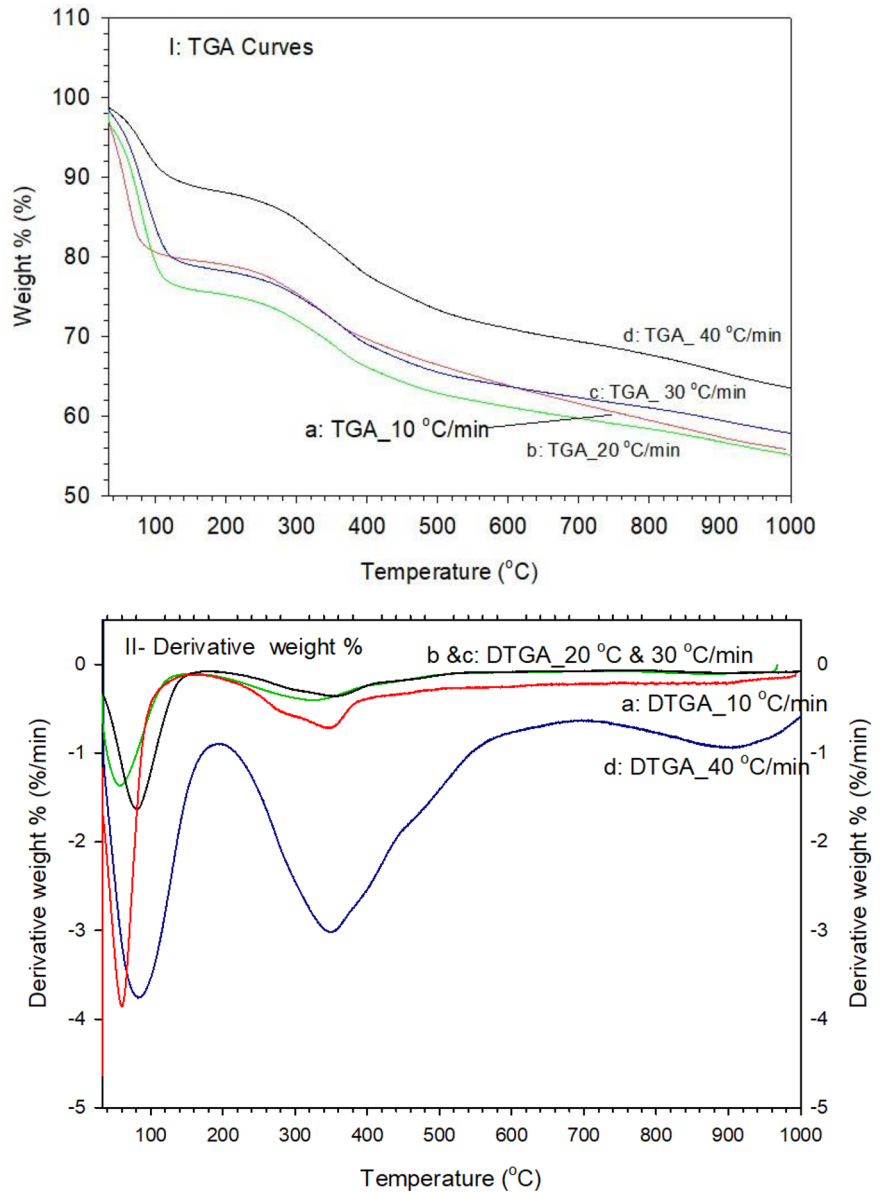
Although determination of total element concentration is important, much more critical is the speciation and bioavailability of elements (Onchoke & Fateru,

2021). This will help determine the extent to which biosolids release elements under various conditions (such as in basic or acidic forms, temperature, organic and/or inorganic mixtures). While not discussed in this research, exposure risks to the environment can be gauged from their redox behavior, individual metal or mixed concentrations, environmental factors such as pH, dissolved oxygen, organic carbon, the presence of sulfides, and cation-ion exchange (Menzie et al., 2009). This will give deeper insight into metal uptake properties by plants, especially when biosolids are applied to land. Risk assessment of biosolids, in East Texas, and globally may be measured by finding out the exposure levels of the metal nanoparticles (Blaisi et al., 2019). As noted (Blaisi et al., 2019), the assessment of the potential risks posed by the ingredients in biosolids (including metals) is necessary. Thus, the measurement of concentrations of pollutants and contaminants including pesticides, pharmaceuticals, and per- and polyfluoroalkyl substances can further be examined before applied to land, incinerated, or sent to landfills.

#### Implications to future research

The comparative metal content of biosolids produced from three wastewater treatment plants in East Texas and a hydroponic material (perlite) commonly used for soil amendments and applications was assessed. These materials contain element concentrations below regulated maximum USEPA ceiling levels. Whereas biosolids can be used in preference to synthesized fertilizers, studies show continuous use thereof over long periods of time may increase soil concentration amounts, particularly for toxic metals such as Cd, Pb, Hg, or Cr. Therefore, continuous evaluations of metal concentrations are required during long periods of land applications. Furthermore, determination of the speciation of the metal concentrations in various biosolids fractions is important. Further research can be focused on determining operative mechanisms through which metal species establish equilibria within soil-biosolids interphases. Such investigations can lead to understanding rates and kinetics of metal release between exchangeable and mobile fractions to soils, and the appropriate dosage amounts for longer application periods. It is also necessary to develop simulation models for the kinetic release mechanisms. Therefore, future research investigations are needed

**Fig. 8** Thermogravimetric and derivative TGA curves of Soil Therapy Compost (STC) heated at 10 °C/min (a) 20 °C/min (b), 30 °C/min (c), and 40 °C/min (d)



in determining the nature of differential interactions between specific metals and humic-mediated release or withholding ability for elements.

**Conclusions**

In summary, characterization of biosolids and a hydroponic material (perlite) by various spectroscopic methods, namely, ICP-OES, FT-IR, SEM, EDX, XRD, and TGA, was investigated. The presence of functional

groups -OH, C=O, and C-H via FT-IR at 3600–3200  $\text{cm}^{-1}$  and 1640  $\text{cm}^{-1}$  implicates the ability of biosolids to complex heavy metals, thus enhancing their uptake and mobility by plants. This is further manifested from SEM micrograph and XRD that show particle size diameters in the range 20–50  $\mu\text{m}$  and extension into the nanocrystalline regime. The observed spectroscopic data including XRD patterns show the presence of crystalline structures vermiculite, alunogen, and quartz in biosolids, which contain elements Ca, Al, and S in their constitution, in accord with ICP-OES and SEM/EDX analyses.

Although total metal content does not provide the full picture on mobility of metals on land applied biosolids, it is nevertheless important for environmental risk assessments. This information is essential to better understanding of disposal effects of biosolids to land while maintaining and restoring soil fertility.

**Acknowledgements** Financial support for research was provided from Stephen F. Austin State University Faculty Research Grants (ORSP # 107552, and Research minigrants) and Robert A. Welch Foundation Grant Number AN-0008. OOF was supported through the Welch and SFASU Chemistry & Biochemistry Department. Special thanks go to Soil and Plant Analysis Lab (SFASU), Nacogdoches and Lufkin Wastewater Treatment Plant facility personnel (Deborah Cassidy, David Wolfgang, and Gary Barton). We thank Professors Josephine Taylor, and Robert Friedfeld for use of SEM/EDX, and X-ray diffractometer. Prof. Alyx Frantzen is thanked for the use of TGA. Any opinions expressed in this paper are those of the authors, and therefore, no official endorsement should be inferred. We thank the Editors and anonymous reviewers whose helpful comments improved the manuscript.

**Author contribution** Kefa K. Onchoke (KKO): Project administration, Conceptualization, Resources, Methodology, Investigation, Data curation, Formal analysis, Validation, Writing-first draft, Writing-original draft, Writing-reviews and editing, Visualization, Supervision, Funding acquisition. Oluwadamilola O Fateru: Formal analysis, Writing-first draft. Robert Friedfeld: Validation, Investigation, Resources (instrumentation), Visualization, Data curation. Wayne Weatherford: Resources, Methodology, Investigation

**Availability of data and material** All data generated or analyzed during this study are included in this published article [and its [Supplementary information](#) files].

## Declarations

**Conflict of interest** The authors declare no competing interests.

## References

- Al-Wabel, M. A., Heil, D. M., Westfall, D. G., & Barbarick, K. A. (2002). Solution chemistry influence on metal mobility in biosolids-amended soils. *Journal of Environmental Quality*, 31(4). <https://doi.org/10.2134/jeq2002.1157>
- APHA. (2013). *Standard methods for the examination of water and wastewater*, 22th ed., American Public Health Association (APHA), American Water Works Association, Water Environment Federation, Washington, DC, 2014. New York: American Public Health Association.
- Barneto, A. G., Carmona, J. A., Martín, J. E., & Blanco, A. J. D. (2009). Kinetic models based in biomass components for the combustion and pyrolysis of sewage sludge and its compost. *Journal of Analytical and Applied Pyrolysis*,

- 86(1), 108–114. <https://doi.org/10.1016/j.jaap.2009.04.011>
- Blaisi, N. I., Clavier, K., Roessler, J., Townsend, T. G., Al-Abed, S. R., & Bonzongo, J.-C.J. (2019). Material- and site-specific partition coefficients for beneficial use assessments. *Environmental Science & Technology*, 53(16), 9626–9635. <https://doi.org/10.1021/acs.est.9b01756>
- Chen, C., Unrine, J. M., Judy, J. D., Lewis, R. W., Guo, J., McNear, D. H., Jr., & Tsyusko, O. V. (2015). Toxicogenomic responses of the model legume medicago truncatula to aged biosolids containing a mixture of nanomaterials (TiO<sub>2</sub>, Ag, and ZnO) from a pilot wastewater treatment plan. *Environmental Science & Technology*, 49(49), 8759–8768. <https://doi.org/10.1021/acs.est.5b01211>
- Cheng, F., Luo, H., Hu, L., Yu, B., Luo, Z., & Cortalezzi, M. F. (2016). Sludge carbonization and activation: from hazardous waste to functional materials for wastewater. *Journal of Environmental Chemical Engineering*, 4(4, Part A), 4574–4586. <https://doi.org/10.1016/j.jece.2016.11.013>
- Cheng, S., Gao, X., Cao, L., Wang, Q., & Qiao, Y. (2020). Quantification of total organic carbon in ashes from smoldering combustion of sewage sludge via a thermal treatment -TGA method. *ACS Omega*, 5(51), 33445–33454. <https://doi.org/10.1021/acsomega.0c05426>
- Choo, K.-H., & Lee, C.-H. (1998). Hydrodynamic behavior of anaerobic biosolids during crossflow filtration in the membrane-aerobic bioreactor. *Water Research*, 32(11), 3387–3397. [https://doi.org/10.1016/S0043-1354\(98\)00103-1](https://doi.org/10.1016/S0043-1354(98)00103-1)
- D'Agostino, L. A., & Mabury, S. A. (2017). Certain perfluoroalkyl and polyfluoroalkyl substances associated with aqueous film forming foam are widespread in Canadian surface waters. *Environmental Science & Technology*, 51(23), 13603–13613. <https://doi.org/10.1021/acs.est.7b03994>
- Fayiga, A. O., & Saha, U. K. (2017). Nanoparticles in biosolids: Effect on soil health and crop growth. *Peertechz Journal of Environmental Science and Toxicology* 2(1), 059–067. <https://doi.org/10.17352/aest.000013>
- Fullana, A. S., Conesa, J. A., Font, R., & Sidhu, S. (2004). Formation and destruction of chlorinated pollutants during sewage sludge incineration. *Environmental Science & Technology*, 38(10), 2953–2958. <https://doi.org/10.1021/es034896u>
- Ghimire, U., Sarpong, G., & Gude, V. G. (2021). Transitioning wastewater treatment plants toward circular economy and energy sustainability. *ACS Omega*, 2021(6), 11794–11803. <https://doi.org/10.1021/acsomega.0c05827>
- Han, N., & Thompson, M. L. (1999). Copper-binding ability of dissolved organic matter derived from anaerobically digested biosolids. *Journal of Environmental Quality*, 28(3), 939–944. <https://doi.org/10.2134/jeq1999.00472425002800030026x>
- Hettiarachchi, G. M., Scheckel, K. G., Ryan, J. A., Sutton, S. R., & Newville, M. (2006). m-XANES and m-XRF investigations of metal binding mechanisms in biosolids. *Journal of Environmental Quality*, 35, 342–351. <https://doi.org/10.2134/jeq2004.0259>
- Islam, K. R., Ahsan, S., Barik, K., & Aksakal, E. L. (2013). Biosolid impact on heavy metal accumulation and lability in soil under alternate-year no-till corn-soybean rotation. *Water Air Soil Pollut*, 224, 1451–1461. <https://doi.org/10.1007/s11270-013-1451-2>

- Keller, A. S., Jimenez-Martinez, J., & Mitrano, D. M. (2020). Transport of nano- and microplastic through unsaturated porous media from sewage sludge application. *Environmental Science & Technology*, *54*(2), 911–920. <https://doi.org/10.1021/acs.est.9b06483>
- Kengne, I. M., Akoa, A., & Koné, D. (2009). Recovery of biosolids from constructed wetlands used for faecal sludge dewatering in tropical regions. *Environmental Science & Technology*, *43*(17), 6816–6821. <https://doi.org/10.1021/es803279y>
- Kiser, M. A., Westerhoff, P., Benn, T., Wang, Y., Pérez-Rivera, J., Hristovski, K. (2009). Titanium nanomaterial removal and release from wastewater treatment plants. *Environmental Science & Technology*, *43*(17), 6757–6763. <https://doi.org/10.1021/es901102n>
- Kreutter, W., Liu, Z., McNamara, P., & Singer, S. (2019). Kinetic analysis of dried biosolid pyrolysis. *Energy & Fuels*, *33*(9), 8766–8776. <https://doi.org/10.1021/acs.energyfuels.9b01911>
- Li, M., Xiao, B., Wang, X., & Liu, J. (2015). Consequences of sludge composition on combustion performance derived from thermogravimetry analysis. *Waste Management*, *35*, 141–147. <https://doi.org/10.1016/j.wasman.2014.10.004>
- Ling, Y. P., Tham, R. H., Siew-Ming Lim, Fahim, M., Ooi, C. H., Krishnan, P., Yeoh, F. Y. (2017). Evaluation and reutilization of water sludge from fresh water processing plant as a green clay substituent. *Applied Clay Science*, *143*, 300–306. <https://doi.org/10.1016/j.clay.2017.04.007>
- Magdziarz, A., & Wilk, M. (2013). Thermal characteristics of the combustion process of biomass and sewage sludge. *Journal of Thermal Analysis and Calorimetry*, *114*, 519–529. <https://doi.org/10.1007/s10973-012-2933-y>
- McConnell, D. B., Shiralipour, A., & Smith, W. H. (1993). Compost application improves soil properties. *Biocycle*, *4*(4), 61–63.
- Menzie, C. A., Ziccardi, L. M., Lowney, Y. W., Fairbrother, A., Shock, S. S., Tsuji, J. S., & Yost, L. J. (2009). Importance of considering the framework principles in risk assessment for metals. *Environmental Science & Technology*, *43*(22), 8478–8482. <https://doi.org/10.1021/es9006405>
- Mtshali, J. S., Tiruneh, A. T., & Fadiran, A. O. (2014). Characterization of sewage sludge generated from wastewater treatment plants in Swaziland in relation to agricultural uses. *Resources and Environment*, *4*(4), 190–199. <https://doi.org/10.5923/j.re.20140404.02>
- Onchoke, K. K., & Fateru, O. O. (2021). Evaluating bioavailability of elements in municipal wastewater sludge (Biosolids) from three rural wastewater treatment plants in East Texas (USA) by a sequential extraction procedure. *Results in Chemistry*, *3*, 100211. <https://doi.org/10.1016/j.rechem.2021.100211>
- Onchoke, K. K., Franclemont, C. M., & Weatherford, P. W. (2018a). Structural characterization and evaluation of municipal wastewater sludge (biosolids) from two rural wastewater treatment plants in East Texas. *USA Spectrochimica Acta A*, *204*, 514–524. <https://doi.org/10.1016/j.saa.2018.06.096>
- Onchoke, K. K., Franclemont, C. M., & Weatherford, P. W. (2018b). Data on ion composition and X-ray diffraction patterns of biosolids from wastewater treatment plants in Lufkin and Nacogdoches, Texas, USA. *Data In Brief*, *20*, 880–888. <https://doi.org/10.1016/j.dib.2018.08.087>
- Onchoke, K. K., Franclemont, C. M., & Weatherford, P. W. (2018c). Data on ion composition and X-ray diffraction patterns of biosolids from wastewater treatment plants in Lufkin and Nacogdoches, Texas, USA. *Data In Brief*, *20*, 880–888. <https://doi.org/10.1016/j.dib.2018.08.087>
- Peccia, J., & Westerhoff, P. (2015). We should expect more out of our sewage sludge. *Environmental Science & Technology*, *49*(14), 8271–8276. <https://doi.org/10.1021/acs.est.5b01931>
- Piotrowski, E. G., Valentine, K. M., & Pfeffer, P. E. (1984). Solid-state, <sup>13</sup>C, cross-polarization, “magic-angle” spinning, NMR spectroscopy studies of sewage sludge. *Soil Science*, *137*(3), 194–203. <https://doi.org/10.1097/0001694-198403000-00010>
- Rengel, Z. (2002). *Handbook of plant growth: pH as the master variable* CRC Press.
- Sherburne, J. J., Anaya, A. M., Fernie, K. J., Forbey, J. S., Furlong, E. T., Kolpin, D. W., & Kinney, C. A. (2016). Occurrence of triclocarban and triclosan in an agro-ecosystem following application of biosolids. *Environmental Science & Technology*, *50*(24), 13206–13214. <https://doi.org/10.1021/acs.est.6b01834>
- Shober, A. L., Hesterberg, D. L., Sims, J. T., & Gardner, S. (2006). Characterization of phosphorus species in biosolids and manures using XANES spectroscopy. *Journal of Environmental Quality*, *35*(6), 1983–1993. <https://doi.org/10.2134/jeq2006.0100>
- Smernik, R. J., Oliver, I. W., & Merrington, G. (2003). Characterization of sewage sludge organic matter using solid-state Carbon-13 nuclear magnetic resonance spectroscopy. *Journal of Environmental Quality*, *32*(4), 1516–1522. <https://doi.org/10.2134/jeq2003.1516>
- Socrates, G. (1994). *Infrared characteristic group frequencies*. John Wiley & Sons Inc.
- Tandy, S., Healey, J. R., Nason, M. A., Williamson, J. C., & Jones, D. L. (2009). Heavy metal fractionation during the co-composting of biosolids, deinking paper fibre and green waste. *Bioresource Technology*, *100*, 4220–4226. <https://doi.org/10.1016/j.biortech.2009.02.046>
- Tettamanti, M., Lasagni, M., Collina, E., Sancassani, M., Pittea, D., LPermo, P., & Cariati, F. (2001). Thermal oxidation kinetics and mechanism of sludge from a wastewater treatment plant. *Environmental Science & Technology*, *35*(19), 3981–3987. <https://doi.org/10.1021/es000257x>
- Tou, F., Yang, Y., Feng, J., Niu, Z., Pan, H., Qin, Y., & Hochella, M. F. (2017). Environmental risk implications of metals in sludges from waste water treatment plants: The discovery of vast stores of metal-containing nanoparticles. *Environmental Science & Technology*, *51*(9), 4831–4840. <https://doi.org/10.1021/acs.est.6b0593>
- Urasa, I. T., & Macha, S. F. (1999). Investigation into heavy metal uptake by wastewater sludges. *Water, Air, and Soil Pollution*, *109*, 207–218. <https://doi.org/10.1023/A:1005093600196>
- USEPA. (1996). *EPA Method 3050B: Acid Digestion of Sediments, Sludges, and Soils*. <https://www.epa.gov/homeland-security-research/epa-method-3050b-acid-digestion-sediments-sludges-and-soils>
- USEPA. (2006). *Emerging technologies for biosolid management, EPA-832/R-06-005; U.S. Environmental Protection*

Agency: Washington, DC, 2006; <http://nepis.epa.gov/Exe/ZyPURL.cgi?Dockey=P1006DGM.txt>

- Vemic, M., Bordas, F., Guibaud, G., Joussein, E., Labanowski, J., Lens, P. N. L., & van Hullebusch, E. D. (2015). Mineralogy and metals speciation in Mo rich mineral sludges generated at a metal recycling plant. *Waste Management*, *38*, 303–311. <https://doi.org/10.1016/j.wasman.2014.12.021>
- Westerhoff, P., Lee, S., Yang, Y., Gordon, G. W., Hristovski, K., Halden, R. U., & Herckes, P. (2015). Characterization, recovery opportunities, and valuation of metals in municipal sludges from U.S. wastewater treatment plants nationwide. *Environmental Science & Technology*, *49*(16), 9479–9488. <https://doi.org/10.1021/es505329q>
- Xue, J., Venkatesan, A. K., Wu, Q., Halden, R. U., & Kannan, K. (2015). Occurrence of bisphenol A diglycidyl ethers (BADGEs) and novolac glycidyl ethers (NOGEs) in archived biosolids from the U.S. EPA's Targeted National Sewage Sludge Survey. *Environmental Science & Technology*, *49* (11), 6538–6544. <https://doi.org/10.1021/acs.est.5b01115>
- Yang, Y., Wang, Y., Westerhoff, P., Hristovski, K., & Jin, V. L. (2014). Metal and nanoparticle occurrence in biosolid-amended soils. *Science of The Total Environment*, *485–486*, 441–449. <https://doi.org/10.1016/j.scitotenv.2014.03.122>
- Zhou, L. X., Yang, H., Shen, Q. R., Wong, M. H., & Wong, J. W. C. (2000). Fractionation and characterization of dissolved organic matter derived from sewage sludge and composted sludge. *Environmental Technology*, *21*(7), 765–771. <https://doi.org/10.1080/09593330.2000.9618962>

**Publisher's Note** Springer Nature remains neutral with regard to jurisdictional claims in published maps and institutional affiliations.